Effects of structural disorder on the optical properties of molecular crystals

Joseph Klafter and Joshua Jortner

Department of Chemistry, Tel-Aviv University, Tel Aviv, Israel

(Received 23 June 1977)

In this paper we advance a model for absorption line shapes of Frenkel excitons in molecular crystals, considering the effects of static disorder and of weak exciton–phonon coupling. Our treatment is limited to single-particle excitations located at the bottom of the exciton band. The effects of disorder scattering at zero temperature are handled by applying the average *t* matrix, single-site approximation to a system characterized by a Gaussian distribution of site excitation energies. The simultaneous effects of disorder scattering and of phonon scattering were treated by the introduction of an effective exciton–phonon Hamiltonian, which was subsequently utilized within the framework of the single-site approximation for disorder scattering at finite temperatures. Model calculations of the optical absorption line shapes were performed for a quasi-one-dimensional system. The zero-temperature line shapes are asymmetrically broadened, the high energy edge being close to a Lorentzian, while the low energy edge decreases fast with decreasing energy. This asymmetry disappears at higher temperatures where phonon scattering effects dominate. We propose that the asymmetric low-temperature absorption band in 1, 4-dibromonaphthalene originates from the effects of structural disorder. The asymmetric optical line broadening experimental data for this quasi-one-dimensional system are well accounted for in terms of our theory.

I. INTRODUCTION

There has been considerable interest recently in the electronic states of quasi-one-dimensional molecular crystals.[1–4] In this context extensive studies have been conducted to elucidate the low-temperature optical spectra and the energy transfer mechanisms in the lowest triplet states of some organic crystals, where the exciton band structure is essentially dominated by one-dimensional interaction.[1,2] A notable example involves the excitonic origin of the 1, 4-dibromonaphthalene (DBN) crystal, which exhibits a pronounced asymmetric line broadening at low temperatures. The studies of Hochstrasser and Whiteman[1] and of Burland[2] have demonstrated (see Fig. 1) that at 2 K a very sharp low energy edge is observed, while the high energy portion of the absorption band reveals a Lorentzian type decrease with increasing energy. The origin of this asymmetry is still not understood. Hochstrasser and Whiteman[1] have proposed that as the $\mathbf{k}=0$ is located at the bottom of the exciton band phonons and structural imperfections do not enhance the transition probability below this energy, while on the high energy side exciton–phonon coupling as well as chemical and physical defects contribute to the line broadening. Subsequent work has attributed the asymmetric line broadening to some kind of exciton–phonon coupling,[2(a)] while the recent work of Macfarlane *et al.*[4] provides strong evidence for the crucial role of structural disorder in determining the low-temperature optical properties of 1, 4-DBN. The notion of low-temperature line broadening due to exciton–phonon coupling of a pure excitonic transition, which is located at the bottom of the exciton band, is fraught with considerable difficulties, as in the limit $T=0$ K the exciton–phonon interaction contributes just to a small level shift and does not give rise to line broadening. This leaves us with the effects of structural disorder on the low-temperature line shapes, a problem of considerable interest in the elucidation of the optical properties and energy transfer mechanisms in chemically pure organic molecular cystals.

We propose that the asymmetric low-temperature triplet exciton absorption line shape in 1, 4-DBN originates solely from the effects of structural disorder, which is by no means typical for a quasi-one-dimensional organic solid. Some support to the idea that structural disorder prevails in 1, 4-DBN have been reported by Macfarlane *et al.*,[4] who have observed small strain inhomogeneity in these crystals. There are also experimental data for a finite linewidth of the lowest $\mathbf{k}=0$ Davydov component located at the bottom of the exciton band in three-dimensional molecular crystals,[5,6] which provides evidence for the role of microscopic structural disorder in "pure"

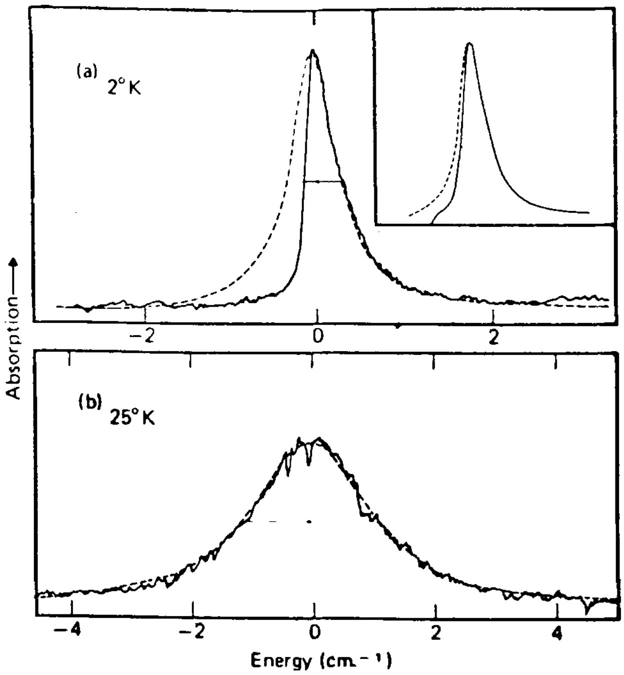

FIG. 1. The experimental absorption line shapes of 1,4-DNB at 2 and 25 K exhibiting the disappearance of the low-temperature asymmetry at high temperature, reproduced from the work of Burland and Macfarlane (Ref. 2).

0021-9606/78/6804-1513$01.00

organic solids. Inhomogeneous broadening of dilute impurity states in mixed molecular crystals is now well documented.[7] Substitutional disorder at low concentrations can result in several distinct trapping sites, each of which exhibits a Gaussian line shape. Typical widths of the distribution of the excitation energies within such a trapping site is 1–5 cm^{-1}.[7] In many chemically pure crystals structural disorder can result in a spread of the zero-order diagonal site excitation energies. To the best of our knowledge the implications of the simultaneous effects of such microscopic structural inhomogeneities and of intermolecular energy transfer in pure crystals were not explored from the theoretical point of view. A closely related problem is that of motional narrowing effects on exciton line shapes in ionic crystals which was studied by Toyozawa and colleagues.[8]

In this paper we advance a model for the absorption line shapes of Frenkel excitons in molecular crystals considering the effects of both structural static disorder and of weak exciton–phonon coupling. We shall limit ourselves to the pure lowest exciton state, i.e., the single-particle excitation, which is located at the bottom of the exciton band. From the point of view of general methodology the present study elucidates the physical implications of simultaneous scattering of excitons by phonons and by static disorder from the microscopic point of view. The only previous study which attempted to provide a description of exciton–phonon together with exciton–disorder scattering involves the interesting stochastic model of Ohata.[9] The theory will be applied for numerical calculations of the optical properties of one-particle excitations in quasi-one-dimensional organic solids. We shall demonstrate that the low-temperature pure exciton linewidth is asymmetric due to the dominating role of disorder scattering, as experimentally observed for triplet excitons in 1, 4-DBN, while at higher temperatures exciton–phonon scattering effects are expected to provide the major contributions for the line broadening.

II. MODEL HAMILTONIAN

We consider Frenkel excitons in a molecular crystal subjected to microscopic perturbations involving both exciton–phonon scattering and exciton scattering by static structural disorder. The model Hamiltonian is

$$H = H_0 + H_1 + H_2, \qquad \text{(II. 1)}$$

where

$$H_0 = \langle\epsilon\rangle \sum_n a_n^+ a_n + \sum_{n<m} J_{nm} a_n^+ a_m + \sum_{\mathbf{q}} \omega_{\mathbf{q}} b_{\mathbf{q}}^+ b_{\mathbf{q}}, \qquad \text{(II. 2a)}$$

$$H_1 = N^{-1/2} \sum_{\mathbf{k},\mathbf{q}} F(\mathbf{k}, \mathbf{q})(b_{\mathbf{q}} + b_{-\mathbf{q}}^+) a_{\mathbf{k}+\mathbf{q}}^+ a_{\mathbf{k}}, \qquad \text{(II. 2b)}$$

$$H_2 = \sum_n \Delta_n a_n^+ a_n. \qquad \text{(II. 2c)}$$

$a_n^+(a_n)$ is the creation (annihilation) operator of the exciton on site n and $a_{\mathbf{k}}^+ = N^{-1/2}\sum_n \exp(i\mathbf{k}\cdot\mathbf{n})\, a_n$, and $b_{\mathbf{q}}^+(b_{\mathbf{q}})$ is the creation (annihilation) operator of a lattice phonon of energy $\omega_{\mathbf{q}}$ and wave vector $\mathbf{q}$. $\langle\epsilon\rangle$ represents the average electronic excitation energy of a molecule in the crystal, while the site excitation energies are $\epsilon_n = \langle\epsilon\rangle + \Delta_n$; the deviations Δ_n of the excitation energies on site n from the mean value are due to structural disorder which affects the local spectral shift (the Davydov D type) terms. H_1 represents the exciton–phonon coupling, while H_2 incorporates the effect of static disorder. We invoke the following assumptions:

(a) The exciton–phonon interaction H_1 is weak,[10] modifying only the transfer integrals J_{nm}. Such weak exciton–phonon coupling is manifested in the absence of phonon sidebands, as is the case for the triplet exciton in 1,4-DBN. This assumption concurs with the recent conclusions of Hanson.[11]

(b) The spread of the local site excitation energies is represented by a Gaussian distribution

$$P(\Delta_1, \Delta_2, \ldots, \Delta_n \cdots) = \prod_n p(\Delta_n),$$

$$p(\Delta_n) = (2\pi D^2)^{-1/2} \exp(-\Delta_n^2/2D^2), \qquad \text{(II. 3)}$$

where D corresponds to the width of the distribution. The probability function (II. 3) was suggested by Sumi and Toyozawa[12] for strong exciton–phonon coupling but, contrary to their treatment, in the present case D is independent of temperature. We assert that there is no correlation between the randomly distributed site energies. Thus, H_2 describes an Anderson type[13] Gaussian disorder.

(c) The transfer integrals J_{nm} are assumed, for the sake of simplicity, to be unaffected by structural disorder.

(d) The exciton bandwidth $2B$ is sufficiently wide to allow for intraband one-phonon-assisted scattering, i.e.,

$$2B > \omega, \qquad \text{(II. 4)}$$

where $\omega \simeq \langle\omega_{\mathbf{q}}\rangle$ is a typical lattice phonon frequency. For the lowest triplet exciton band in 1, 4-DBN $2B \cong 28\ \mathrm{cm}^{-1}$ while lattice phonon frequencies with $\omega = 17\ \mathrm{cm}^{-1}$ were identified, whereupon the condition (II. 4) is obeyed. Accordingly, one-phonon terms are expected to provide a dominating contribution to the self-energy. When the condition (II. 4) is violated one-phonon scattering does not prevail and high-order effects such as Raman type two-phonon processes have to be incorporated.

(e) We consider one-particle excitations and have not included two-particle excitations. This requires the consideration of the intramolecular phonons and their interaction with electronic excitations. In view of the high frequencies of the intramolecular vibrations the one-particle excitations are well separated in energy from the two-particle excitations which can be treated separately.

(f) For the sake of simplicity we consider a crystal structure consisting of one molecule per unit cell. This approach is adequate also for triplet excitons in the anisotropic crystal of 1, 4-DBN which are quasi-one-dimensional.

(g) The $\mathbf{k} = 0$ exciton state is assumed to be located at the bottom of the exciton band.

The absorption line shape, apart from an irrelevant numerical constant, is given by[10]

$$I(E) = -\mathrm{Im}\,\langle G(\mathbf{k}=0,\ E)\rangle_c, \quad \mathbf{k}=0 \tag{II.5}$$

being expressed in terms of the retarded Green's function[10]

$$G(\mathbf{k},\ E) = \int e^{-iEt} \ll a_{\mathbf{k}}(t);\ a^{+}_{\mathbf{k}}(0) \gg dt, \tag{II.6}$$

where the sympol $\ll\ \gg$ represents thermal averaging over the canonical ensemble of phonon states, and $\langle\ \rangle_c$ denotes configurational averaging over the disorder field. It is well known[10] that the effects of an external "bath" on the free exciton Green's function can be accounted for by the introduction of a (complex) self-energy $\Sigma(\mathbf{k},\ E)$, so that

$$\langle G(\mathbf{k},\ E)\rangle_c = [E - E_{\mathbf{k}} - \Sigma(\mathbf{k},\ E)]^{-1}. \tag{II.7}$$

The line shape [Eq. (II.5)] is

$$I(E) = \frac{-\mathrm{Im}\,\Sigma(0,\ E)}{[E - E_{\mathbf{k}} - R_e\Sigma(0,\ E)]^2 + [\mathrm{Im}\,\Sigma(0,\ E)]^2} \tag{II.8}$$

The self-energy Σ will obviously assume a different form for a phonon bath and for a disorder field (which can also be regarded as a bath). In what follows we shall first consider separately the exciton self-energy for the well-known case of phonon scattering, as well as for disorder scattering, and subsequently proceed to consider the simultaneous effects of lattice phonons and of static disorder.

III. THE SELF-ENERGY AND THE LINE SHAPE

A. Thermal broadening

Considering first only exciton–phonon weak coupling $H = H_0 + H_1$ we shall quote, for the sake of simplicity, the well-known results which retain only the first term in the continued fraction expansion of the self-energy.[10] The self-energy for thermal broadening in the one-phonon scattering approximation is

$$\Sigma^T(\mathbf{k},\ E) = N^{-1}\sum_{\mathbf{q}} |F(\mathbf{k},\ q)|^2 \left(\frac{n_{\mathbf{q}}+1}{E - E_{\mathbf{k+q}} - \omega_{\mathbf{q}}} + \frac{n_{\mathbf{q}}}{E - E_{\mathbf{k+q}} + \omega_{\mathbf{q}}}\right),$$

$$n_{\mathbf{q}} = [\exp(\omega_{\mathbf{q}}/k_B T) - 1]^{-1}. \tag{III.1}$$

At zero temperature

$$\mathrm{Re}\Sigma^T(\mathbf{k}=0,\ E) = PP\sum_{\mathbf{q}} \frac{|F(\mathbf{k}=0,\ \mathbf{q})|^2}{E - E_{\mathbf{q}} - \omega_{\mathbf{q}}}, \tag{III.2a}$$

$$\mathrm{Im}\Sigma^T(\mathbf{k}=0,\ E) = -\pi\sum_{\mathbf{q}} |F(\mathbf{k}=0,\ \mathbf{q})|^2\, \delta(E - E_{\mathbf{q}} - \omega_{\mathbf{q}}). \tag{III.2b}$$

The level shift [Eq. (III.2a)] due to phonon scattering is negative at the bottom $E_{\mathbf{k}=0} \simeq -B$ of the exciton band, and we assert that $\mathrm{Im}\Sigma^T(\mathbf{k}=0,\ \bar{E}) = 0$ at $\bar{E} = -B + \mathrm{Re}\Sigma^T(\mathbf{k}=0,\ -B)$. It is apparent from Eq. (II.8) that, provided that polariton[14] effects are disregarded, the absorption line shape is a delta function and no line broadening of the $\mathbf{k}=0$ exciton originating from inelastic exciton–phonon coupling will be exhibited at $T = 0$ K. In the low-temperature regime line broadening of the $\mathbf{k}=0$ exciton can originate from multiphonon intramolecular electronic relaxation, which is trivially small for the lowest triplet state, or from elastic scattering by a disorder field. We now proceed to consider the latter possibility.

B. Structural disorder

We now treat the Anderson Hamiltonian

$$H = H_0 + H_2 \tag{III.3}$$

characterized by Gaussian disorder [Eq. (II.3)] of the site energies. Various schemes have been advanced to provide approximations for the configurationally averaged Green's function, $\langle G(\mathbf{k},\ E)\rangle_c$ when no phonons are included.[15–18] We restrict our treatment to the single-site approximation. We shall use the average t-matrix approximation (ATA) which, in contrast to the coherent potential approximation, is not self-consistent. However, the ATA is simple and yields physically transparent results. It will provide a good insight into the physical features of the inhomogeneous broadening. In what follows we shall provide a derivation of the ATA scheme using the methods advanced by Ziman.[17]

We are interested in the configurational average $\langle G(\mathbf{k},\ E)\rangle_c$, while the unperturbed Green's function $G^0(\mathbf{k},\ E)$ for the exciton is

$$G^0(\mathbf{k},\ E) = \frac{1}{E - E_k + i\eta}, \quad \eta \to 0^+, \tag{III.4}$$

whose local representation is given by

$$G^0_{ll'} = N^{-1}\sum_{\mathbf{k}} \frac{\exp[i\mathbf{k}\cdot(\mathbf{l}-\mathbf{l}')]}{E - E_{\mathbf{k}} + i\eta}. \tag{III.5}$$

Starting with the t-matrix representation and using the definition of the t-matrix,[17]

$$\langle G_{ll'}\rangle_c = G^0_{ll'} + \sum_n G^0_{ln}\langle t_n\rangle_c G^0_{nl'} + \sum_{n\neq m} G^0_{ln}\langle t_n G_{nm} t_m\rangle_c G^0_{ml'} + \cdots, \tag{III.6}$$

where the t matrix in the local-site representation is

$$t_n = \frac{\Delta_n}{1 - \Delta_n G^0_{nm}}. \tag{III.7}$$

We now invoke the assumption

$$\langle t_n^m\rangle_c = \langle t_n\rangle_c^m, \tag{III.8}$$

namely, we neglect the repeated scatterings of an exciton by pairs, triplets, etc., of molecules.[15–18] We then obtain

$$\langle G_{ll'}\rangle_c = G^0_{ll'} + \sum_n G^0_{ln}\langle t_n\rangle_c G^0_{nl'} + \sum_{n\neq m} G^0_{ln}\langle t_n\rangle_c G^0_{nm}\langle t_m\rangle_c G^0_{ml'} + \cdots. \tag{III.9}$$

The configurationally averaged Green's function in the momentum representation is

$$\begin{aligned}\langle G(\mathbf{k},\ E)\rangle_c &= (E - E_{\mathbf{k}} - \Sigma_c)^{-1}\\ &= \frac{1}{[G^0(\mathbf{k},\ E)]^{-1} - \Sigma_c}\\ &= \frac{G^0(\mathbf{k},\ E)}{1 - \Sigma_c G^0(\mathbf{k},\ E)},\end{aligned} \tag{III.10}$$

where Σ_c is the self-energy due to disorder scattering. $\Sigma_c \equiv \Sigma_c(E)$ is energy dependent but not momentum dependent, a feature common to all single-site approximations.[15] A perturbation type expansion of Eq. (III. 10) recast in the local site representation yields

$$\langle G_{II'}\rangle_c = G^0_{II'} + \sum_n G^0_{In}\Sigma_c G^0_{nI'} + \sum_{n,m} G^0_{In}\Sigma_c G^0_{nm}\Sigma_c G^0_{mI} + \cdots , \tag{III. 11}$$

where now the multiple sums involve unrestricted labels. Equations (III. 9) and (III. 11) result in

$$\langle t_n\rangle_c = \frac{\Sigma_c}{1 - G^0_{nn}\Sigma_c}, \tag{III. 12}$$

which leads to the relation

$$\Sigma_c = \frac{\langle t_n\rangle_c}{1 + \langle t_n\rangle_c G^0_{nn}}. \tag{III. 13}$$

Utilizing the definition (III. 7) we obtain the following expression for the self-energy:

$$\left\langle \frac{1}{[G^0_{nn}]^{-1} - \Delta_n}\right\rangle_c = \frac{1}{[G^0_{nn}]^{-1} - \Sigma_c}. \tag{III. 14}$$

Equation (III. 14) constitutes the ATA result. The energy dependence of the self-energy thus obtained is responsible for the asymmetry in the line shape.

The ATA equation (III. 14) will now be recast for the normal probability distribution (II. 3) of the site excitation energies

$$\int_{-\infty}^{\infty} \frac{p(\Delta_n)}{[G^0_{nn}]^{-1} - \Delta_n}\, d\Delta_n = \frac{1}{[G^0_{nn}]^{-1} - \Sigma_c}. \tag{III. 15}$$

Integrating Eq. (III. 15) we obtain

$$-i\pi^{1/2}\exp(-[G^0_{nn}]^{-2}/2D^2)[1 - \mathrm{erf}(-i[G^0_{nn}]^{-1}/\sqrt{2}D)] = \frac{1}{[G^0_{nn}]^{-1} - \Sigma_c}, \tag{III. 16}$$

where erf(Z) is the error function of a complex argument. Equation (III. 16) results in an explicit expression for the self-energy

$$\Sigma_c = [G^0_{nn}]^{-1} - \{-i(\pi/2)^{1/2} D^{-1}\exp(-[G^0_{nn}]^{-2}/2D^2) \times [1 - \mathrm{erf}(-i[G^0_{nn}]^{-1}/\sqrt{2}D)]\}^{-1}. \tag{III. 17}$$

It is apparent from this result that the self-energy is related to the Green's function of the ideal lattice which can be determined from the density of states.

It will be useful at this stage to understand how elastic scattering of excitons by disorder modifies the optical absorption line shape. Considering an unperturbed exciton band spanning the energy range $-B \leq E \leq B$ it was shown by Sumi and Toyozawa[12] (see Appendix A) that an expansion of Eqs. (III. 16) or (III. 17) for $D^2/B^2 \ll 1$ inside the band ($E > -B$) results in a perturbation type result in

$$\Sigma_c(E) = D^2 G^0_{nn}(E), \qquad E > -B, \tag{III. 18}$$

where the Green's function is complex. Outside the band ($E < -B$) one gets for small values of D/B

$$\Sigma_c(E) = \mathrm{Re}\Sigma_c(E) + i\,\mathrm{Im}\,\Sigma_c(E), \qquad E < -B,$$
$$\mathrm{Re}\Sigma_c(E) = D^2 G^0_{nn}(E),$$
$$\mathrm{Im}\Sigma_c(E) = -(\pi/2)^{1/2} D^{-1}[G^0_{nn}(E)]^{-2}\exp(-[G^0_{nn}]^{-2}/2D^2), \tag{III. 19}$$

where $G^0_{nn}(E)$ is real. This different behavior of the self-energy inside and outside the original unperturbed band results in the origin of the asymmetry of the low-temperature absorption line shape

$$I(E) = \frac{-\mathrm{Im}\Sigma_c(E)}{[E + B - \mathrm{Re}\Sigma_c(E)]^2 + [\mathrm{Im}\Sigma_c(E)]^2}, \tag{III. 20}$$

where $E_{k=0} = -B$ is located at the bottom of the exciton band. Inside the band $\mathrm{Im}\Sigma_c(E) = -D^2\pi\rho_0(E)$, where $\rho_0(E)$ is the density of the exciton states in the ideal crystal. Provided that the self-energy [and $\rho_0(E)$] does not vary too fast with E, an assumption which we shall show in Sec. IV is even applicable for a quasi-one-dimensional system, we get

$$I(E) \cong \frac{\pi D^2\rho_0(E)}{(E - E)^2 + [\pi D^2\rho_0(E)]^2}, \qquad E > -B, \tag{III. 21}$$

with $\bar{E} = -B - R_e\Sigma_c(E)$. Thus, the line shape inside the original exciton band exhibits a Lorentzian (or a modified Lorentzian) energy dependence. On the other hand, outside the exciton band edge when $|E + B| \gg |R_e\Sigma_c(E)|$ the line shape is

$$I(E) \cong \frac{-\mathrm{Im}\Sigma_c(E)}{(E + B)^2}, \qquad E < -B. \tag{III. 22}$$

The energy dependence of the self-energy determines the fast decrease of $I(E)$ with decreasing E outside the band. This energy dependence of $I(E)$ is being determined according to Eq. (III. 19) by the unperturbed (real) Green's function and thus by the density $\rho_0(E)$ of exciton states. This brings up an interesting feature which pertains to the dependence of the low energy tail of the absorption band on the dimensionality of the exciton band structure. For a three-dimensional system we have demonstrated elsewhere that the low energy absorption band $E < -B$ is characterized by an Urbach tail.[19] For a quasi-one-dimensional band structure, which is the subject matter of the present work, we take first a simple one-dimensional unperturbed density of states function

$$\rho_0(E) = \begin{cases} \pi^{-1}(B^2 - E^2)^{1/2}, & |E| < B, \\ 0, & |E| > B, \end{cases} \tag{III. 23}$$

and the Green's function is

$$G^0_{nn}(E) = -(E^2 - B^2)^{-1/2}. \tag{III. 24}$$

From Eqs. (III. 19), (III. 22), and (III. 23) we obtain outside the exciton band

$$I(E) \propto (E + B^3(E - B)\exp[-(E^2 - B^2)/2D^2]. \tag{III. 25}$$

Equation (III. 25) exhibits an exponential decrease of the low energy tail of $I(E)$ with E^2 for a one-dimensional system. From the foregoing analysis, based on Eqs. (III. 21) and (III. 25), we can provide a proper rationalization for asymmetric line broadening in a quasi-one-dimensional system which originates from disorder scattering

C. Simultaneous effects of phonon scattering and disorder scattering

We now consider exciton states in a molecular crystal which are affected by structural disorder as well as by coupling with the phonon states. Such a state of affairs coexists at finite temperatures where both scattering channels will prevail. We have now to perform a double average of the Green's function [Eq. (II. 5)] accounting both for thermal averaging and for configurational averaging, a problem which is by no means trivial. To accomplish this goal we shall assume that the phonon field is not perturbed by structural disorder so that only the electronic excitations are affected by the disorder field. We are well aware of the fact that decoupling approximations may be fraught with considerable difficulties and pitfalls.[20] However, in the present case we are interested in rather weak exciton scattering by the disorder field i.e., $D/B<1$, where $2B$ is the exciton bandwidth. Exciton localization will then be exhibited over a small energy range in the vicinity of $E=-B$, and even in that energy region the localization length[21] will be large, extending over many lattice sites. According to Anderson[22] the nature of the exciton–phonon (or exciton–electron) interaction depends on the localization length. Exciton–phonon coupling in the states near $E=-B$ is expected to be weak due to their almost extended nature.

We now introduce a two-step effective field approximation. In the first step we replace the phonon field by an effective complex field, which results in an exciton–phonon effective Hamiltonian. In the second stage this effective exciton–phonon Hamiltonian is utilized within the framework of a single-site approximation to account for disorder scattering. In Appendix B we demonstrate that this approximation is equivalent to the decoupling of the effects arising from the interaction between phonon scattering and disorder scattering. The analysis of Appendix B also demonstrates that one should account first for the effects of the phonon field and subsequently for the effect of disorder, as carried out by us, rather than applying the two-step effective-field approximation in a reverse order.

To proceed to the outline of our two-step effective-field approximation we first replace the phonon field by the self-energy $\Sigma^T(\mathbf{k}, E)$, which is given by Eq. (III. 1). The effective exciton–phonon Hamiltonian is

$$H^T_{\text{eff}} = \langle\epsilon\rangle \sum_n a_n^+ a_n + \sum_{n<m} J_{nm} a_n^+ a_m + \sum_n \Delta_n a_n^+ a_n + \sum_{n<m} \Sigma^T_{nm}(E) a_n^+ a_m, \tag{III. 26a}$$

which can be recast in the form

$$H^T_{\text{eff}} = \sum_{\mathbf{k}} [E_{\mathbf{k}} + \Sigma^T(\mathbf{k}, E)] a_{\mathbf{k}}^+ a_{\mathbf{k}} + \sum_n \Delta_n a_n^+ a_n, \tag{III. 26b}$$

where

$$\Sigma^T_{nm}(E) = N^{-1} \sum_{\mathbf{k}} \exp[i\mathbf{k}(\mathbf{n}-\mathbf{m})\Sigma^T(\mathbf{k}, E)] \tag{III. 27}$$

is the exciton–phonon self-energy in the site representation. This completes the first stage of the treatment. In the second step we are interested in the configurationally averaged Green's function

$$\langle G(k, E)\rangle_c = \left\langle \frac{1}{E - H^T_{\text{eff}}} \right\rangle_c = \frac{1}{E - E_k - \Sigma(\mathbf{k}, E)}, \tag{III. 28}$$

where

$$\Sigma(\mathbf{k}, E) = \Sigma^T(\mathbf{k}, E) + \Sigma_c(E) \tag{III. 29}$$

is the total self-energy corresponding to the exciton–phonon-disorder system, which consists of the phonon self-energy Σ^T and the disorder self-energy Σ_c. To derive an explicit expression for Σ_c we can now follow the ATA scheme developed in Sec. III. B, replacing the zero-order Green's function G^0_{ll} [Eq. (III. 5)] by

$$g^0_{ll}(E) = N^{-1} \sum_{\mathbf{k}} \frac{1}{E - E_{\mathbf{k}} - \Sigma^T(\mathbf{k}, E)}. \tag{III. 30}$$

The ATA equation (III. 14) is replaced by

$$\left\langle \frac{1}{[g^0_{nn}(E)]^{-1} - \Delta_n} \right\rangle_c = \frac{1}{[g^0_{nn}(E)]^{-1} - \Sigma_c}, \tag{III. 31}$$

while the final expression for the self-energy is obtained by replacing Eq. (III. 17) with

$$\Sigma_c = \sqrt{2}Dz - \{-i(\pi/2)^{1/2} D^{-1} \exp(-z^2)[1 - \operatorname{erf}(-iz)]\}^{-1}, \quad z = [g^0_{nn}]^{-1}/\sqrt{2}D. \tag{III. 32}$$

It is apparent for Eq. (III. 32) that Σ_c is energy dependent and, furthermore, as this self-energy is determined by $g^0_{nn}(E)$ [Eq. (III. 32)] we assert that $\Sigma_c = \Sigma_c[E, \Sigma^T(\mathbf{k}, E)]$ is determined also by the exciton–phonon self-energy. Within the framework of the Einstein, single frequency approximation for the lattice phonons which we shall subsequently utilize both Σ^T and $\Sigma_c(E, \Sigma_T)$ are only energy dependent being independent of **k**. The absorption line shape is now obtained from Eqs. (III. 29), (III. 30), (III. 32), and (II. 5) as

$$I(E) = \frac{-\operatorname{Im}[\Sigma^T(E) + \Sigma_c(E)]}{\{E - E_{\mathbf{k}=0} - \operatorname{Re}[\Sigma^T(E) + \Sigma_c(E)]\}^2 + \{\operatorname{Im}[\Sigma^T(E) + \Sigma_c(E)]\}^2}, \tag{III. 33}$$

which constitutes our final result.

IV. MODEL CALCULATIONS

We shall now apply the ATA scheme for the calculation of the optical properties of the lowest one-particle excitation in a model system where the ideal (unperturbed) exciton band is characterized by a quasi-one-dimensional density of states. A natural choice for the unperturbed density of states in a one-dimensional system involves Eq. (III. 23). However the systems we are concerned with, i.e., triplet excitons in 1, 4-DBN, are not strictly one dimensional, as there is always some finite, though small, interchain coupling. Accordingly, we modify the one-dimensional density of states by adding a small phenomenological width ϵ to the energy which will smear the one-dimensional sharp Van Hove singularities, and we take

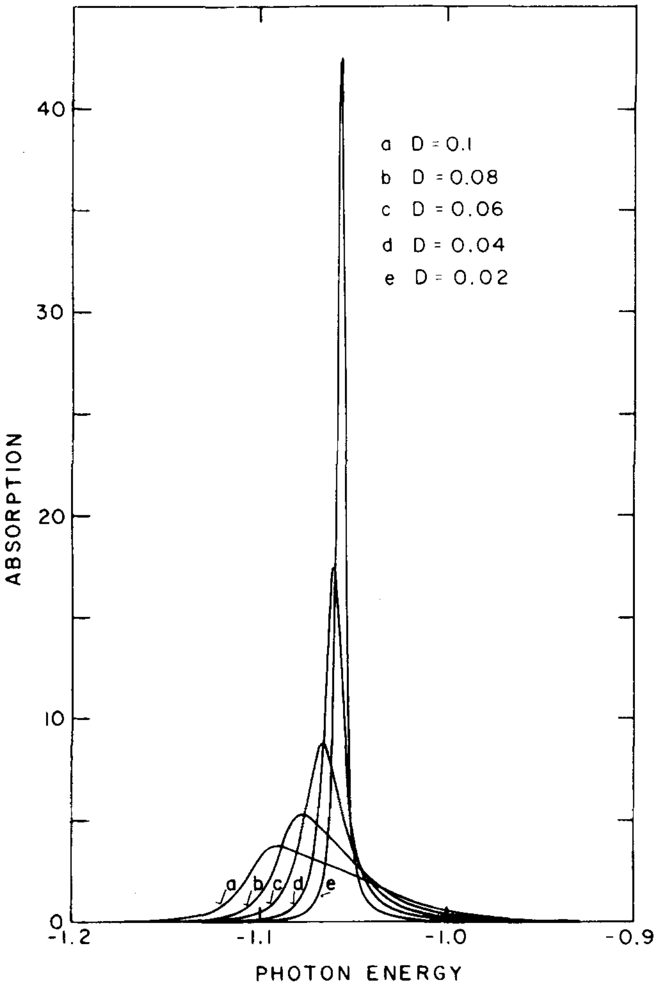

FIG. 2. Effects of structural disorder on the absorption line shapes of a quasi-one-dimensional system. Calculations were done for $|F|^2=0.1$, $\omega=1.0$, and $kT=0$ (in units of B).

$$\rho_0(E)=\begin{cases}\frac{1}{\pi}\mathrm{Re}[B^2-(E+i\epsilon)^2]^{-1/2}, & |E|<B,\\ 0, & |E|>B,\end{cases} \tag{IV.1}$$

where $\epsilon\approx 10^{-3}$–10^{-2}. Numerical calculations show that our results for the optical absorption line shape are invariant on the choice of ϵ/B in that region. In view of the small value of D/B we can still safely assume that $E_{k=0}=-B$ is located at the bottom of the exciton band.

We now consider the low-temperature absorption line shapes. In Fig. 2 we portray the model calculations of the line shapes at $T=0$ K for several values of D/B, which exhibits the following features:

(a) Disorder scattering results in an increase of the linewidth with increasing D. In Fig. 3(a) we present the linewidth at half-maximum $(\mathrm{FWHM})=E_l-E_r$, where E_l and E_r represent the energies at half the band maximum in the high and in the low energy range, respectively. It is apparent from Fig. 3(a) that $(\mathrm{FWHM})\propto D^2$.

(b) The low-temperature absorption line shapes in the quasi-one-dimensional system are asymmetrically broadened, as is evident from Fig. 2. The high energy edge is close to a Lorentzian in accordance with Eq. (III.21). The low energy edge decreases fast with decreasing energy, as expected from Eq. (III.22). To provide a quantitative measure of the asymmetry we define the asymmetry factor

$$\eta=\delta_r/\delta_l, \tag{IV.2}$$

where $\delta_r=E_{\max}-E_r$ and $\delta_l=E_l-E_{\max}$, $E_{\max}$ being the energy of the peak absorption band. The asymmetry factor at low temperature is presented in Fig. 3(b).

(c) Disorder scattering results in a shift of the band maximum from the unperturbed value for the ideal excitonic transition which should peak at $E_{\max}=-B$. This is a simple level shift effect originating from $\mathrm{Re}\Sigma(E)$ in Eq. (III.19). Theoretical results for this level shift effect are presented in Fig. 3(c), where we portray $E_{\max}$ vs D/B.

To investigate the optical properties at finite temperature we have to incorporate now the simultaneous effects of phonon coupling and disorder scattering, according to Eqs. (III.28)–(III.33) and (IV.1). In Fig. 4 we portray typical results obtained for $D/B=0.1$, for several values of the exciton–phonon coupling parameter $|F/B|^2=0.01$, 0.05, 0.1 for the effective lattice phonon frequency $\omega/B=1$ and $kT=0, 1$. The results of Fig. 4 clearly demon-

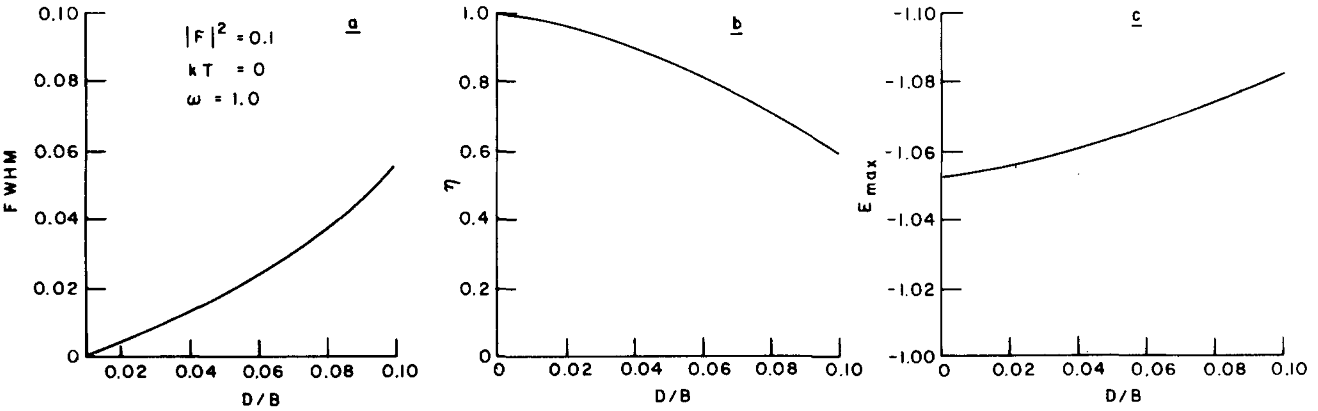

FIG. 3. The disorder effects on the following: (a) full line width at half maximum (FWHM), (b) asymmetry parameter η, (c) maximum peaks position $E_{\max}$. (a)–(c) are portrayed as functions of the disorder parameter D for $|F|^2=0.1$, $\omega=1$, and $kT=0$ (in units of B).

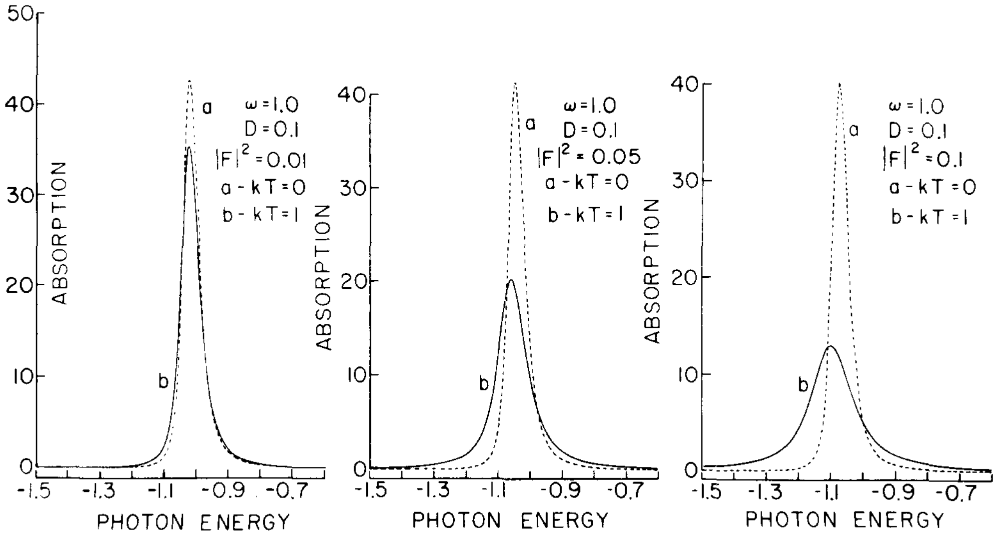

FIG. 4. Simultaneous effects of structural disorder and of weak exciton–phonon coupling. Phonon energy is $\omega = 1$, $kT = 0$ and 1 for three values of $|F|^2$ (in units of B).

strate that the asymmetric line broadening exhibited at low temperatures may disappear at higher temperatures. In the higher-temperature regime phonon broadening dominates, resulting in almost symmetric Lorentzian-type absorption line shapes. To provide some quantitative information regarding the "transition" from the "low-temperature" regime where disorder scattering prevails to the "high-temperature" regime where phonon scattering dominates, we note the following:

(d) The FWHM is temperature independent for $0 < kT < 0.2B$, as is evident from Fig. 5(a). In the low-temperature range the FWHM is almost independent of the phonon coupling strength. For $kT > 0.2B$ a phonon like line broadening sets in and we expect $(\mathrm{FWHM}) \propto \mathrm{cotg}(h\omega/2k_kT)$, as is the case for weak coupling.

(e) The asymmetry factor [Eq. (IV.2)] is practically constant in the temperature range $kT = 0 - 0.2B$, increasing towards the value of $\eta = 1$, corresponding to a symmetric line shape, with increasing temperature [Fig. 5(b)]. As expected the increase of η towards unity is enhanced at higher values of the exciton–phonon coupling parameter.

(f) The band maximum $E_{\max}$ is shifted towards lower energies below $E = -B$. The level shift originating from $\mathrm{Re}\Sigma$ is due to the combined effects of phonons and disorder and is negative and finite at $T = 0$ K in Fig. 5(c). At higher temperatures for $kT > 0.2B$ the position of the band maximum shifts to lower energies with increasing T. This effect originates from the temperature dependence of $\mathrm{Re}\Sigma^T$ [Eq. (III.19)], which contributes to the $I(E)$ in Eq. (III.20).

We now confront these theoretical predictions with the available experimental data for triplet excitons in 1,4-DBN. The general features of the low-temperature 2 K experimental absorption line shape which exhibits a Lorentzian high energy portion for $E > E_{\max}$ are in accord with Eq. (III.21) and a sharp drop at the low energy side which is consistent with Eq. (III.22). In 1,4-DBN $2B \cong 28$ cm^{-1}, according to the results of Hochstrasser and Whiteman.[1] Raman spectroscopy has identified a phonon frequency at $\omega = 17$ cm^{-1},[2] so the value of $\omega = B \cong 15$ cm^{-1} utilized in our calculations is reasonable. The low-temperature (2 K) spectra result in[1,2] (FWHM) = 0.7 cm^{-1}, i.e., (FWHM)/B = 0.05 and $\eta = 0.6$. An examination of Figs. 3 and 5 reveals that both these experimental parameters can be adequately accounted for in terms of disorder scattering with $D/B \cong 0.1$. Thus, the spread of local site excitation energies is $D \cong 1.5$ cm^{-1}, a reasonable value which may be considerably lower than the Davydov local-site shift term. Triplet exciton states are ideal candidates to probe the effects of structural

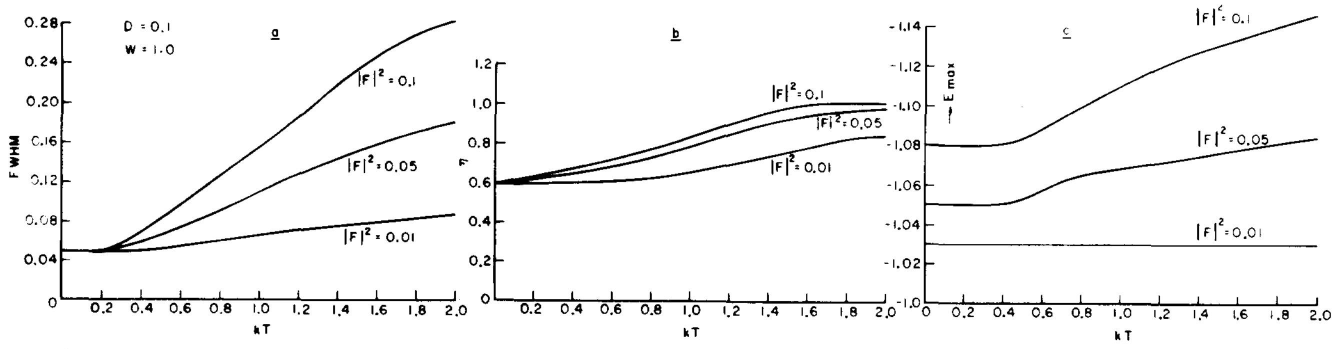

FIG. 5. Simultaneous contributions of structural disorder and of weak exciton–phonon coupling to the following: (a) FWHM, (b) asymmetry parameter η, (c) maximum peaks position $E_{\max}$. (a)–(c) are given as functions of kT for different values of $|F|^2$. $\omega = 1$, $D = 0.1$ (all energies in units of B).

disorder in organic crystals as they are characterized by a moderately narrow exciton band $B \leq 100$ cm^{-1} and small values of D may result in dramatic effects on the absorption line shapes at low temperatures. At 20 K ($kT = 1.1B$) (FWHM) = 3.0 cm^{-1}, i.e., (FWHM)/B = 0.20, which, according to Fig. 5(a), results in the value $|F|^2 \cong 0.05-0.1$ for the exciton–phonon coupling strength. At this higher temperature the theoretical asymmetry factor is $\eta = 1$ and the line shape is expected to be due to a Lorentzian, in agreement with the experimental results of Burland.[2]

V. CONCLUDING REMARKS

We have explored the effects of structural disorder on the optical properties of organic molecular crystals with a special reference to the absorption line shapes in quasi-one-dimensional exciton bands. The theory presented herein is not restricted to the quasi-one-dimensional case. Any exciton band effects of disorder scattering on the absorption line shape corresponding to the lowest one-particle excitation exhibit the following universal features: (1) finite linewidth at $T = 0$ K, (2) asymmetric line broadening is exhibited at $T = 0$ K, (3) the high energy edge of the absorption band at $T = 0$ K is expected to be close to a Lorentzian, according to Eq. (III.21), and (4) the low energy edge will be "sharp," according to Eq. (III.22). The functional energy dependence of the low energy portion of the absorption band is determined by the dimensionality of the exciton band structure. For a three-dimensional exciton band structure disorder scattering will result in a temperature independent low energy Urbach tail.[19] In a quasi-one-dimensional system the Urbach tail will not be observed and the gross features of the low energy tail are expected to follow the functional dependence given by Eq. (III.25).

The quantitative analysis of the triplet excitons in 1,4-DBN provides strong support for our proposal that incorporation of positional structural disorder is crucial in the understanding of the low-temperature optical properties of chemically pure organic solids. We assert that the physical features of exciton states in the low-temperature domain $kT < 0.2B(\sim 0.2\omega)$, where ω is a typical lattice phonon energy, drastically differ from the characteristics of the high-temperature region where phonon scattering dominates. The effects of structural disorder will be crucial for a quantitative understanding of a variety of low-temperature physical phonemena pertaining to electronic excitations in molecular crystals, such as polariton effects, electron spin resonance and nuclear spin resonance of exciton states, as well as energy transfer processes, all of which have to be carefully re-examined whenever experimental evidence from structural data or from the analysis of optical properties becomes available for a specific system.

The model calculations for the low-temperature absorption line shape of quasi-one-dimensional exciton states have a wide applicability also for electronic excitations in other materials, such as organic and inorganic polymers. Extensive studies were recently conducted in an attempt to understand the electronic structure of several polydiacetylene polymers.[3] The lowest-lying absorption band of these polymers, located at about ~1.5 eV, exhibits a pronounced asymmetry at low temperature, revealing again a sharp low-energy edge. This asymmetric line shape was originally assigned to a one-dimensional band to band transition.[3a] However, recent photoconductivity studies demonstrate that the onset of the band to band transition occurs at ~0.5 eV above the lowest 2.5 eV absorption band[23] which has to be assigned to an excitonic transition. We suggest that the asymmetric line shape observed in quasi-one-dimensional polydiacetylene chains may originate from the effects of structural disorder.[3b]

The results of the present study provide the first step towards the quantitative understanding of the effects of structural disorder on exciton dynamics and energy transfer processes in molecular solids. In this context we recall that the starting point of the present analysis of optical line shapes rests on the reasonable assumption of a Gaussian distribution of the diagonal site excitation energies, in analogy to inhomogeneous broadening of single impurity states. Intermolecular energy transfer, manifested in terms of the transfer integrals J_{nm}, results in a distortion of the line shape from the Gaussian distribution of the site excitation energies. We would like to mention that asymmetric absorption line shapes are a consequence of general effects of disorder and do not pertain just to positional disorder, as substitutional disorder results in similar characteristics[24] of the lineshapes. In general, the asymmetry of the absorption line shapes and, in particular, the sharp low-energy edge is substitutionally disordered and in positionally disordered organic solids can be attributed to the contribution of low-lying states located in the low energy portion of the density of states. When the exciton band structure is dominated by short-range interactions these states in the tails of the band will be localized. This brings us to the discussion of some qualitative features of Anderson–Mott localization theory[13] and its applicability to energy transfer in (disordered) organic crystals. For a one-dimensional system Mott and Twose[25] have demonstrated that diagonal disorder will result in localization. However, for excitons in quasi-one-dimensional organic solids, such as triplet states in 1,4-DBN, small interchain coupling prevails and exciton localization has to be treated in terms of an extension of Anderson's model to incorporate anisotropic interactions, an unsolved problem which is of considerable interest. In quasi-two-dimensional and three-dimensional positionally disordered chemically pure systems exciton localization can be considered by the application of Anderson's theory.[13] It was predicted by Anderson that for a system where the diagonal excitation energies exhibit inhomogeneous broadening localization of the excitation can occur provided that the intermolecular transfer integrals fall faster than dipole–dipole coupling and when the spread (D) of the site excitation energies is sufficiently large relative to the exciton bandwidth. There have been some recent very interesting experimental studies which point towards a critical concentration for localization of excitation energy at low temperatures for transition localization of excitation energy at low temperatures for transition metal ions in ionic crystals.[26]

The effects of microscopic structural inhomogeneities on energy transfer and on exciton localization in organic crystals can be experimentally explored by similar studies of energy resolved spectra of molecular crystals excited by a narrow band laser. These interesting problems deserve further theoretical and experimental studies.

ACKNOWLEDGMENT

This research was completed while one of the authors (J. Jortner) was a Sherman Fairchild Distinguished Scholar at the California Institute of Technology. He is indebted to the Division of Chemistry and Chemical Engineering, California Institute of Technology, for its hospitality.

APPENDIX A. DERIVATION OF EQS. (III.18) and (III.19)

Starting from Eq. (III. 16) we define

$$Z=[G^0_{nn}]^{-1}/\sqrt{2}D. \tag{A1}$$

Equation (III. 16) is now rewritten in the form

$$-i\pi^{1/2}\exp(-z^2)[1-\mathrm{erf}(-iz)]=\frac{1}{[G^0_{nn}]^{-1}-\Sigma_c}. \tag{A2}$$

We are interested in the limit $D^2/B^2 \ll 1$, namely, when $|z^2| \gg 1$.

We now treat the energy range inside the unperturbed density of states, and the energy range outside the density of states separately.

(a) $E > -B$. In this region z is complex. Using the asymptotic expansion of $\mathrm{erf}(-iz)=1-\mathrm{erf}(-iz)$ we get[27]

$$1/\sqrt{2}D^{-1}z^{-1}[1+z^{-2}/2+0(z^{-4})]$$
$$=\frac{1}{[G^0_{nn}]^{-1}-\Sigma_c}\,\frac{1}{\sqrt{2}Dz-\Sigma_c}. \tag{A3}$$

Expanding the RHS of Eq. (A3) we obtain

$$(1/\sqrt{2})D^{-1}z^{-1}(1+z^{-2}/2+\cdots)=(1/\sqrt{2})D^{-1}z^{-1}\left(\frac{1}{1-\Sigma_c/\sqrt{2}Dz}\right)$$
$$=(1/\sqrt{2})D^{-1}z^{-1}[1+(1/\sqrt{2})D^{-1}z^{-1}\Sigma_c+\cdots], \tag{A4}$$

and therefore

$$\Sigma_c=(1/\sqrt{2})Dz^{-1}=D^2G^0_{nn}(E). \tag{A5}$$

(b) $E < -B$. In this energy range z is real. Rewriting the LHS of Eq. (A2) in terms of the real and imaginary parts we get

$$\begin{aligned}\mathrm{Re}(\mathrm{A2})&=i(\pi/2)^{1/2}D^{-1}\exp(-z^2)\,\mathrm{erf}(-iz),\\ \mathrm{Im}(\mathrm{A2})&=-(\pi/2)^{1/2}D^{-1}\exp(-z^2).\end{aligned} \tag{A6}$$

Utilizing the same expansion of the RHS of Eq. (A3) it follows that

$$\mathrm{Re}\Sigma_c=D^2G^0_{nn}(E),$$
$$\mathrm{Im}\Sigma_c=-(\pi/2)^{1/2}D^{-1}[G^0_{nn}]^{-2}\exp(-[G^0_{nn}]^{-2}/2D^2). \tag{A7}$$

APPENDIX B. DECOUPLING APPROXIMATION

We shall demonstrate the equivalence of the two-step effective-field approximation and the decoupling of phonon scattering and disorder scattering, using the equation of motion method for the Green's function.[10,28]

In the momentum representation

$$\sum_n \Delta_n a_n^+ a_n = N^{-1}\sum_{\mathbf{k}\mathbf{k}'}\Delta_{\mathbf{k},\mathbf{k}'}a_{\mathbf{k}}^+ a_{\mathbf{k}'}, \tag{B1}$$

where

$$\Delta_{\mathbf{k},\mathbf{k}'}=\sum_n \exp[i(\mathbf{k}-\mathbf{k}')\cdot\mathbf{n}]\Delta_n. \tag{B2}$$

The Green's function is defined in Eq. (II.6). Following Zubarev[10,28] the equations of motion for the exciton and phonon operators are

$$i\frac{da_{\mathbf{k}}}{dt}=E_{\mathbf{k}}a_{\mathbf{k}}+N^{-1/2}\sum_{\mathbf{q}}F^*(\mathbf{k},\mathbf{q})\,a_{\mathbf{k}+\mathbf{q}}(b_{\mathbf{q}}^++b_{-\mathbf{q}})+N^{-1}\sum_{\mathbf{k}'}\Delta_{\mathbf{k},\mathbf{k}'}a_{\mathbf{k}'},$$
$$i\frac{db_{\mathbf{q}}}{dt}=\omega_{\mathbf{q}}b_{\mathbf{q}}+N^{-1/2}\sum_{\mathbf{k}}F(\mathbf{k},-\mathbf{q})\,a_{\mathbf{k}-\mathbf{q}}^+a_{\mathbf{k}},$$
$$-i\frac{db_{\mathbf{q}}^+}{dt}=\omega_{\mathbf{q}}b_{\mathbf{q}}^++N^{-1/2}\sum_{\mathbf{k}}F(\mathbf{k},\mathbf{q})\,a_{\mathbf{k}+\mathbf{q}}^+a_{\mathbf{k}}. \tag{B3}$$

The equation of motion for the retarded Green's function $G(k, t)$ is

$$i\frac{dG(\mathbf{k},t)}{dt}=\delta(t)+E_{\mathbf{k}}G(\mathbf{k},t)$$
$$+N^{-1/2}\sum_{\mathbf{q}}F^*(\mathbf{k},\mathbf{q})\{P_1+P_2\}+N^{-1}\sum_{\mathbf{k}'}\Delta_{\mathbf{k},\mathbf{k}'}G(\mathbf{k}',t), \tag{B4}$$

$$P_1\equiv P_1(\mathbf{k}+\mathbf{q},\mathbf{q},\mathbf{k};t)=\langle\langle a_{\mathbf{k}+\mathbf{q}}^{(t)}\,b_{\mathbf{q}}^+(t);\ a_{\mathbf{k}}^+(0)\rangle\rangle,$$
$$P_2\equiv P_2(\mathbf{k}+\mathbf{q},\mathbf{q},\mathbf{k};t)=\langle\langle a_{\mathbf{k}+\mathbf{q}}^{(t)}\,b_{-\mathbf{q}}^{(t)};\ a_{\mathbf{k}}^+(0)\rangle\rangle. \tag{B5}$$

In the equation of motion for P_1 and P_2[10,28] we neglect the disorder contribution, assuming no correlation between the phonon field and the disorder field. According to Zubarev[28] and Davydov[10] we get

$$\begin{aligned}&[E-E_{\mathbf{k}}-\Sigma^T(\mathbf{k},E)]G(\mathbf{k},E)=1+N^{-1}\sum_{\mathbf{k}'}\Delta_{\mathbf{k},\mathbf{k}'}G(\mathbf{k}',E),\\ &[E-E_{\mathbf{k}}-\Sigma^T(\mathbf{k},E)]=g^{-1}(\mathbf{k};E).\end{aligned} \tag{B6}$$

$\Sigma^T(\mathbf{k},E)$ is given by Eq. (III. 1)[10] or

$$G(\mathbf{k},E)=g(\mathbf{k},E)+N^{-1}g(\mathbf{k},E)\sum_{\mathbf{k}}\Delta_{\mathbf{k}\mathbf{k}'}G(\mathbf{k}',E). \tag{B7}$$

In the site representation

$$G_{nm}(E)=g_{nm}(E)+\sum_l g_{nl}(E)\Delta_l\,G_{lm}(E). \tag{B8}$$

The next step in our treatment involves the ATA approximation starting with

$$g_{nm}(E)=N^{-1}\sum_{\mathbf{k}}\frac{\exp[i\mathbf{k}(\mathbf{n}-\mathbf{m})]}{E-E_{\mathbf{k}}-\Sigma^T(\mathbf{k}\ \ E)} \tag{B9}$$

and proceeding with the treatment of Sec. III.C.

[1] R. M. Hochstrasser and J. D. Whiteman, J. Chem. Phys. 56, 5945 (1972).

[2] (a) D. M. Burland, J. Chem. Phys. 59, 4283 (1973); (b) D.

M. Burland and R. M. Macfarlane, J. Lumin. **12**, 213 (1976).
[3](a) D. Bloor, Chem. Phys. Lett. **42**, 174 (1976); (b) D. Bloor, W. Hersel, and D. N. Batchelder, Chem. Phys. Lett. **45**, 411 (1977).
[4]R. M. Macfarlane, U. Konzelman, and D. M. Burland, J. Chem. Phys. **65**, 1022 (1976).
[5]A. Brillante and L. A. Dissado, Chem. Phys. **12**, 297 (1976).
[6]K. Tomioka, M. Animoto, T. Tomotika, and A. Matsui, J. Chem. Phys. **59**, 4157 (1973).
[7](a) H. deVries and D. A. Wiersma, Phys. Rev. Lett. **36**, 91 (1976); (b) A. H. Zewail and T. E. Orlowski, Chem. Phys. Lett. **45**, 399 (1977); (c) T. Artsma and D. A. Wiersma, Chem. Phys. Lett. **42**, 520 (1976).
[8]Y. Toyozawa, in *Vacuum Ultraviolet Radiation Physics*, edited by E. E. Koch, R. Haensel, and C. Kunz (Pergamon, London, 1974).
[9]N. Ohata, Prog. Theor. Phys. **51**, 1332 (1974).
[10]A. S. Davydov, in *Theory of Molecular Excitons* (Plenum, New York, 1971).
[11]D. Hanson, Chem. Phys. Lett. **43**, 217 (1976).
[12]H. Sumi and Y. Toyozawa, J. Phys. Soc. Jpn. **31**, 342 (1971).
[13]P. W. Anderson, Phys. Rev. **109**, 1492 (1958).
[14]S. Robinette and G. Small, J. Chem. Phys. **65**, 837 (1976).
[15]B. Velicky, S. Kirkpatrick, and H. Ehrenreich, Phys. Rev. 175, 747 (1968).
[16]F. Brouers, J. Phys. C **4**, 773 (1971).
[17]J. M. Ziman, J. Phys. C 2, 1230 (1969).
[18]Y. Onodera and Y. Toyozawa, J. Phys. Soc. Jpn. **24**, 341 (1968).
[19]J. Klafter and J. Jortner, "Urbach Rule in the Optical Spectra of Crystalline and Amorphous Organic Solids" Chem. Phys. (in press).
[20]J. Klafter and J. Jortner, "Two-Particle Excitations in Molecular Crystals" (to be published).
[21]E. N. Economou and C. Papatriantafillou, Solid State Commun. **11**, 197 (1972).
[22]P. W. Anderson, Nature (London) **235**, 163 (1972).
[23]R. R. Chance and R. H. Boughman, J. Chem. Phys. **64**, 3889 (1976).
[24]J. Hoshen and J. Jortner, J. Chem. Phys. **56**, 5550 (1972).
[25]N. F. Mott and W. D. Twose, Adv. Phys. **10**, 107 (1961).
[26]S. K. Lyo, Phys. Rev. B **3**, 3331 (1971).
[27]M. Abramowitz and I. A. Stegun, in *Handbook of Mathematical Functions*, (Dover, New York, 1968).
[28]D. N. Zubarev, Sov. Phys. Usp. **3**, 320 (1960).